

# Comparison of the AVI, modified SINTACS and GALDIT vulnerability methods under future climate-change scenarios for a shallow low-lying coastal aquifer in southern Finland

Samrit Luoma<sup>1</sup> · Jarkko Okkonen<sup>2</sup> · Kirsti Korkka-Niemi<sup>3</sup>

Received: 14 February 2016 / Accepted: 28 August 2016 / Published online: 26 September 2016  
© The Author(s) 2016. This article is published with open access at Springerlink.com

**Abstract** A shallow unconfined low-lying coastal aquifer in southern Finland surrounded by the Baltic Sea is vulnerable to changes in groundwater recharge, sea-level rise and human activities. Assessment of the intrinsic vulnerability of groundwater under climate scenarios was performed for the aquifer area by utilising the results of a published study on the impacts of climate change on groundwater recharge and sea-level rise on groundwater–seawater interaction. Three intrinsic vulnerability mapping methods, the aquifer vulnerability index (AVI), a modified SINTACS and GALDIT, were applied and compared. According to the results, the degree of groundwater vulnerability is greatly impacted by seasonal variations in groundwater recharge during the year, and also varies depending on the climate-change variability in the long term. The groundwater is potentially highly vulnerable to contamination from sources on the ground surface during high groundwater recharge rates after snowmelt, while a high vulnerability to seawater intrusion could exist when there is a low groundwater recharge rate in dry season. The AVI results suggest that a change in the sea level will have an insignificant impact on

groundwater vulnerability compared with the results from the modified SINTACS and GALDIT. The modified SINTACS method could be used as a guideline for the groundwater vulnerability assessment of glacial and deglacial deposits in inland aquifers, and in combination with GALDIT, it could provide a useful tool for assessing groundwater vulnerability to both contamination from sources on the ground surface and to seawater intrusion for shallow unconfined low-lying coastal aquifers under future climate-change conditions.

**Keywords** Aquifer vulnerability · Vulnerability mapping · Climate change · Coastal aquifer · Finland

## Introduction

Shallow permeable aquifers located in low-lying coastal areas are vulnerable not only to contamination from sources that are located on the ground surface, but also to seawater intrusion and/or flooding of coastal areas either due to sea-level rise or storm surges (e.g. Luoma and Okkonen 2014; Luoma et al. 2013; Oude Essink 1999, 2001; Barlow 2003; Pulido-Leboeuf 2004; Oude Essink et al. 2010; Rasmussen et al. 2013; Ferguson and Gleeson 2012; Ataie-Ashtiani et al. 2013). These events will presumably be accelerated by the changing climate, including changes in precipitation, temperature and groundwater recharge, as well as sea-level rise and an increasing frequency of storm surges (IPCC 2000, 2007; Nicholls et al. 2007). Besides these, the increasing demand for water by the population and industry, as well as changing land-use practises as a result of human activities, could expose shallow aquifers to contamination.

The intrinsic vulnerability of an aquifer is the relative degree of natural protection of an aquifer from contamination by anthropogenic sources at the land surface. It is defined as a

✉ Samrit Luoma  
samrit.luoma@gtk.fi

Jarkko Okkonen  
jarkko.okkonen@gtk.fi

Kirsti Korkka-Niemi  
kirsti.korkka-niemi@helsinki.fi

<sup>1</sup> Geological Survey of Finland, P.O. Box 96, FI-02151 Espoo, Finland

<sup>2</sup> Geological Survey of Finland, P.O. Box 97, FI-67101 Kokkola, Finland

<sup>3</sup> Department of Geosciences and Geography, University of Helsinki, P.O. Box 64, FI-00014 Helsinki, Finland

function of the hydrogeological characteristics of the aquifer, without considering the type and intensity of human activities at the surface (Vrba and Zaporozec 1994). Although the vulnerability of an aquifer to contamination is based not only on hydrogeological factors but also on land-use factors (Vrba and Zaporozec 1994), the hydrogeological factors would not change appreciably over time, whereas land use would. For the sustainable and effective management and protection of groundwater resources, an intrinsic vulnerability assessment should be performed for any aquifer area, as an indicator of aquifer vulnerability and the need for detailed investigations. Particularly in low-lying permeable coastal aquifers, where the groundwater level is close to the ground surface, a small increase in groundwater recharge and sea-level rise may increase aquifer vulnerability.

A shallow aquifer in the Hanko area in southern Finland, the case study area, is confronting these issues, and there is an attempt to maintain water supply quality within the drinking-water standards in the long term. Referring to Luoma and Okkonen (2014), a rise in the sea level due to global climate change would cause some parts of the Hanko aquifer to be below the sea level, compromising groundwater quality. This, together with the predicted increase in precipitation, would increase groundwater recharge and raise the water table, consequently contributing to the potential deterioration of groundwater quality or potential flooding in the low-lying aquifer area.

A number of methods have been used to assess the intrinsic vulnerability of aquifers. Among these, DRASTIC (Aller et al. 1987), SINTACS (Civita 1994), GOD (Foster 1987) and the AVI (Van Stempoot et al. 1993) are well-known and suitable methods for aquifers in clastic sedimentary environments. The DRASTIC method is usually used to determine the vulnerability of groundwater to contamination from anthropogenic sources from the ground surface. However, it does not take into account factors associated with watercourses such as lakes or rivers that are connected to the aquifer. SINTACS is a modified DRASTIC method with more options for the weight strings, including additional factors associated with human activities and watercourses, while the rating system of each parameter is still preserved as in the original DRASTIC method. For coastal aquifers, however, both DRASTIC and SINTACS have no parameters to determine contamination from seawater intrusion, which is a different and more complicated process compared with contamination via sources from the ground surface (Werner et al. 2013).

The GALDIT index (Chachadi et al. 2003; Lobo-Ferreira et al. 2007), a system of weights and ratings similar to DRASTIC and SINTACS, is a well-known method for assessing the vulnerability to seawater intrusion of coastal aquifers. The GALDIT vulnerability index map indicates the aquifer area along the coastline that is most likely to be affected by seawater intrusion and provides recommendations for detailed site investigations of aquifer areas. Although

GALDIT does not take into account the rate of groundwater withdrawal relative to the total amount of freshwater recharge to the aquifer, or the freshwater–saltwater interface in the seawater intrusion process, the simplicity of this method makes it attractive for assessing aquifer vulnerability to seawater intrusion (Ivkovic et al. 2013), and it has been used for many coastal aquifer areas around the world (e.g. Chachadi et al. 2003; Chachadi and Lobo-Ferreira 2007; Lobo-Ferreira et al. 2007; Dörfliger et al. 2011; Najib et al. 2012; Kura et al. 2015; Recinos et al. 2015). According to the National Research Council (1993), vulnerability assessment methods must be evaluated in order to verify the assigned vulnerability rating and increase the reliability of assessments. However, for all of the afore-mentioned methods, only a few cases have reported the validation of the method, and the most commonly used method has been a comparison of the results with geochemical data from groundwater samples (Allouche et al. 2015). The distribution of indicators of seawater intrusion such as total dissolved solids (TDS), Cl and the Na/Cl ratio, and the extent of the freshwater–seawater interface from the Ghyben-Herzberg model have also been compared with the GALDIT vulnerability index maps (Trabelsi et al. 2016).

In Finland, the shallow groundwater resides in Quaternary sediments deposited during the Weichselian glaciation and deglaciation. The sediments consist of glacial gravel, sand, till and clay, and in some areas with postglacial littoral gravel, sand and clay. The aquifer areas are very often located next to watercourses such as lakes or rivers (Okkonen and Kløve 2010) or human infrastructure (e.g. urban areas, industries, highways). Lavapuro et al. (2008) modified the DRASTIC method to assess the intrinsic vulnerability of an aquifer in an esker deposit where the sediments mainly consist of gravel and sand. This modified DRASTIC method nevertheless did not represent the overall depositional patterns of the shallow aquifers in Finland, where the deposits consist not only of esker material (with the deposition of coarse-grained sediments, e.g. gravel and sand), but also of ice-marginal end formations (with the deposition of gravel, sand, glacial till, silt and clay layers) or postglacial littoral sediments (gravel, sand and clay). A vulnerability assessment method that can be applied for the whole depositional environment of shallow groundwater areas such as in Finland, as mentioned in the previous section, and a method that can provide the same standard for all shallow aquifers, is still needed.

Although SINTACS appears better suited than DRASTIC to the vulnerability assessment of shallow glaciogenic aquifers, the rating classifications in SINTACS are still not representative of the depositional environments of shallow groundwater areas—for example, the aquifer media of such areas do not include basalt or massive sandstone or limestone. In this study, the rating classification of SINTACS was modified for three parameters: the soil media, aquifer media and the attenuation capacity of the unsaturated zone based on the

superficial deposit map of Finland. The aim was to make it more suitable for aquifers formed in glacial deposits and depositional environments following deglaciation.

This study examined how the impacts of climate change on groundwater recharge, sea-level rise and the water table affect the vulnerability of the shallow low-lying coastal glaciogenic aquifer in Hanko, southern Finland. The results of a previous assessment of climate change impacts on the Hanko aquifer by Luoma and Okkonen (2014) were used to provide the inputs for three index models, the AVI, the modified version of SINTACS and GALDIT, and the results from the models were compared. The numerical approaches could be useful tools to predict contaminant transport in both space and time in the coastal aquifers. However, these approaches often have data and computational demands that are not easy to meet (e.g. Sanford and Pope 2010). A recent study by Beebe et al. (2016) suggests that analytical approaches are not always reliable. If framed properly, index models could be able to support these types of vulnerability assessments. In addition, index models are generally used instead of numerical groundwater flow and transport models for the assessment of the groundwater vulnerability because they are easy to use and the index maps can be simply overlaid and integrated with thematic maps, such as land use and hydrogeological maps, in order to provide information to support the decisions of land users and land-use managers in groundwater risk assessment in the area.

In order to assess the potential impacts of climate change on the vulnerability of an aquifer and its ability to sustain groundwater development in the future, vulnerability index maps under climate variability and change should be prepared and examined, which can be done by first assessing climate change impacts on the aquifer and then using the outcomes in different vulnerability assessment methods. This study applied the outcomes of Luoma and Okkonen (2014) to demonstrate the impacts of climate variability and climate change on aquifer vulnerability. In addition, hydrogeochemical data, as well as field investigation and monitoring data, including the temperature, water level and electrical conductivity (EC) of groundwater, were used to confirm the degree of seawater intrusion and validate the vulnerable areas of the coastal Hanko aquifer. The vulnerability index map was used to assess the vulnerability of groundwater to potential sources of contamination in the groundwater area at present and also those predicted for the future under different climate change scenarios.

## Study area

### Background

The study area is located on the Hanko peninsula on the southern coast of Finland at approximately 59°53'N 23°10'E

(Fig. 1). The shallow, unconfined, low-lying coastal aquifer in Hanko consists of porous gravels and sands of an ice-marginal end deposit, and is located in a low-lying coastal area bounded by the Baltic Sea. It is an important source of drinking water and the water supply for residents of the town Hanko and the local industries. The economy of Hanko town is based on services (61 %) and industry (38 %) and the population in 2016 was 9109 (Hanko 2016). Hanko is a popular summer resort, and the population considerably increases during the summer due to the arrival of holiday homeowners and tourists. The Hanko area belongs to the temperate coniferous-mixed forest climate zone with cold, wet winters. The mean annual temperature is 6 °C, with mean minimum and maximum temperatures of −4.2 and 16.6 °C, respectively. The average annual precipitation was 620 mm during the period 1971–2000. Forestry, mainly of Scots pine (*Pinus sylvestris*), is the main land use in the aquifer area (approximately 80 % of land use). Additionally, the existing potential anthropogenic impacts from human activities in the area, namely gravel excavation pits, local industries and salt (NaCl) used for de-icing on the highway that runs through the middle of the groundwater area, could pose a contamination risk to groundwater quality.

### Geology and hydrogeology

The Quaternary deposits in the Hanko area are underlain by the basement of the Precambrian crystalline igneous and metamorphic rocks (Fig. 2). The Precambrian bedrock mainly consists of granite, quartz diorite and granodiorites, forming a sharp unconformity with the Quaternary deposit with some outcrops in the area (Kielosto et al. 1996). The aquifer in the study area is in the First Salpausselkä ice-marginal formation, deposited during the Weichselian and Holocene deglaciation of the Scandinavian Ice Sheet (Fyfe 1991; Saarnisto and Saarinen 2001). The formation consists of gravel, sand, glacial till, silt and clay, and of postglacial littoral gravel, sand and clay (Fig. 1) that was originally deposited as sub-glacial outwash fan deposits (Fyfe 1991).

The primary ice-marginal formation in Hanko was formed in deep water as a low narrow ridge (Fyfe 1991). When the ice sheet withdrew from the area, this deep-water deposit was covered by fine-grained sediments, silt and clay layers of the Ancylus Lake and Littorina Sea. The sea level has been regressive since deglaciation because of isostatic land uplift. The primary deposit of the First Salpausselkä formation was exposed to sea waves and also to wind (Kielosto et al. 1996). The well-sorted gravels indicate reworked materials from the high energy of waves and storm activities, and are found over a large area in Santala, while the fine sand from aeolian deposits covers a large area in the east (Fig. 1; Fyfe 1991; Kielosto et al. 1996). The lake and wetlands in the middle of the aquifer



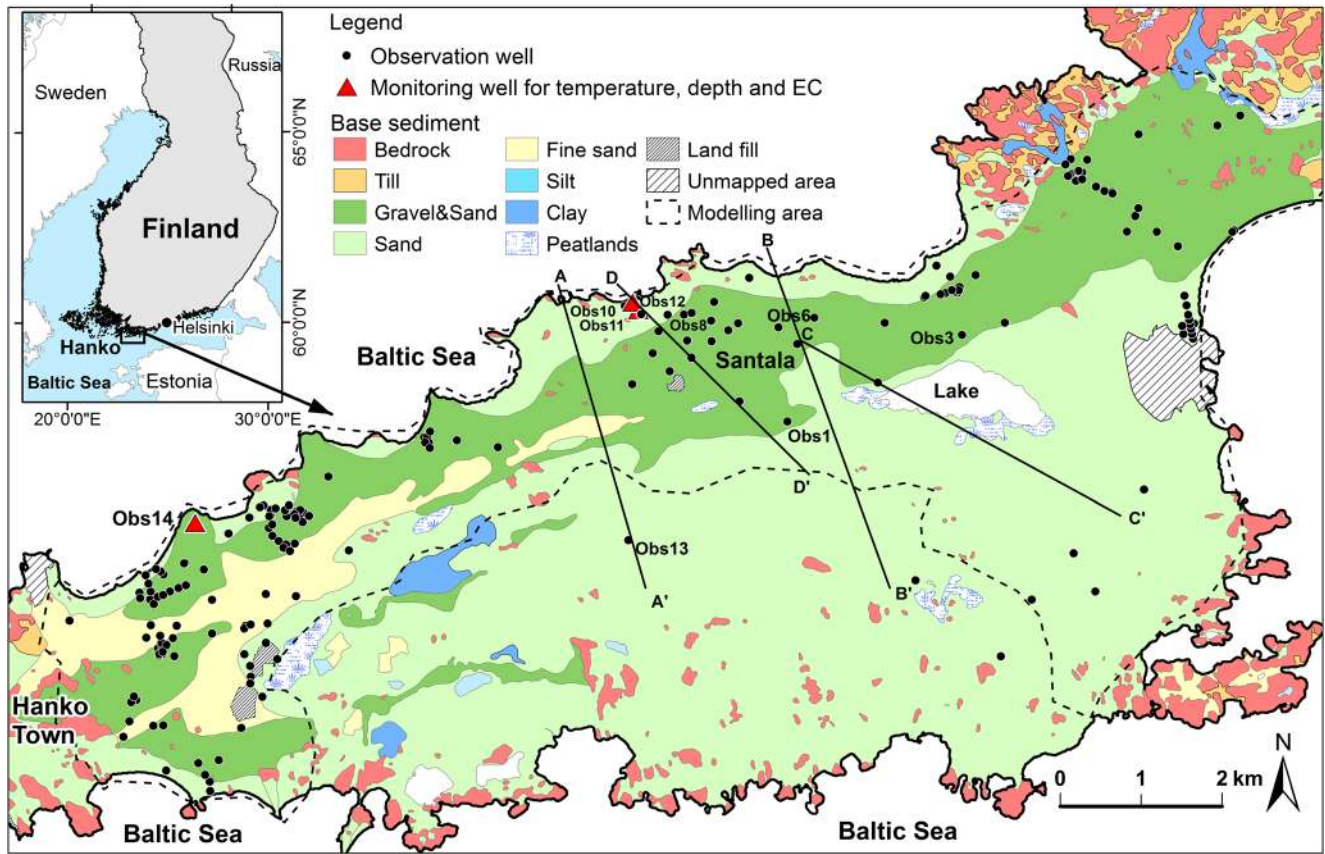
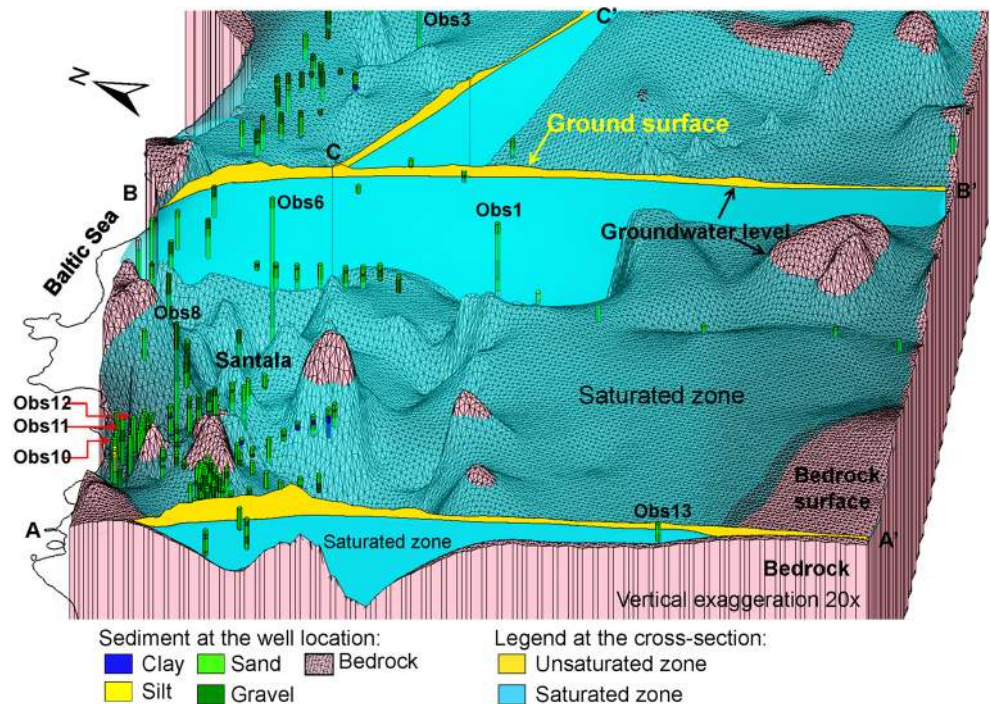


**Fig. 1** Location and Quaternary geological deposit map of the study area in the eastern Baltic Sea region. Cross-section lines A–A’ to C–C’ are presented in Fig. 2 and D–D’ in the last figure

are located in a depression that forms part of the First Salpausselkä formation and the sand dune terrain. The lake

has a surface area of about 1.8 km<sup>2</sup>, with an average depth of approximately 1–2 m.

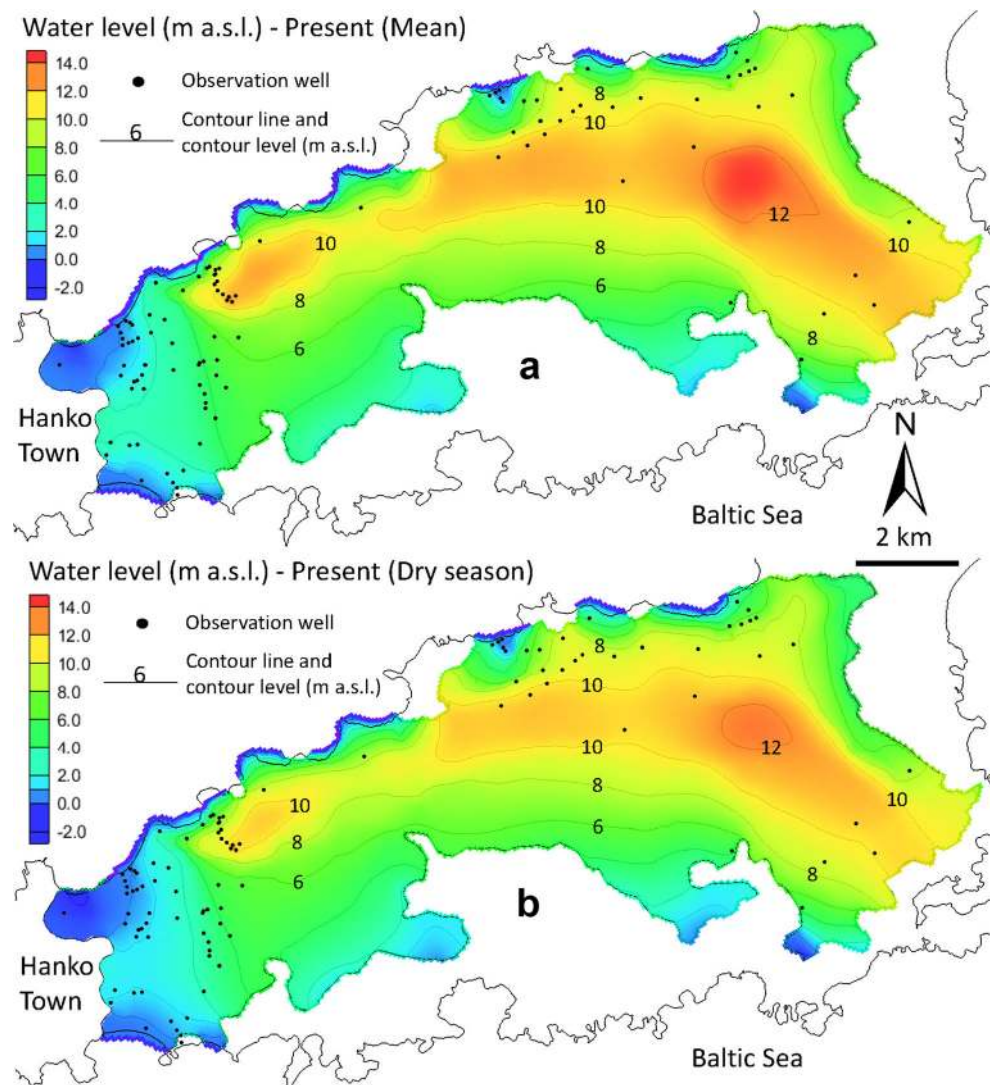
**Fig. 2** Visualisation of the bedrock surface, groundwater level and sediments at drilled wells in the Santala area. Cross-section lines A–A’, B–B’ and C–C’ represent the thicknesses of saturated and unsaturated zones of the Quaternary sediment. The locations of cross-section lines and observation wells (Obs) are indicated in Fig. 1



The topographic landform of the study area varies between 10 and 14 m above sea level (a.s.l.) along the northern ridge of the First Salpausselkä formation, and its elevation decreases to less than 2 m along the northern coastline, while in the south and southeast the elevation gradually decreases to 5–7 m a.s.l. The shallow aquifer in Hanko is unconfined, with the thickness of the Quaternary deposits varying from less than 1–75 m, and the average thickness being about 25 m. The sediments are generally thick on the western side, in a NE–SW direction conforming to the First Salpausselkä formation, and their thickness decreases eastwards to less than 1 m in the eastern coastal area. The simulated groundwater levels under mean and dry (summer) climate conditions at present (1971–2000) are shown in Fig. 3 (Luoma and Okkonen 2014). The water table varies between 2 and 10 m below the ground surface in the inland area, and is less than 2 m below the ground surface in the coastal area, where groundwater discharges into the Baltic Sea. In many parts of

the aquifer, the groundwater level is close to the ground surface, and water intake areas are located along the coastline, where the groundwater level may often fall below the sea level. According to the results of well testing and soil sample analysis, the hydraulic conductivity of the aquifer ranges from 0.3 to 4.8 m day<sup>-1</sup> in silty sand and fine sand, and is up to 100 m day<sup>-1</sup> in sand and gravel (Luoma and Pullinen 2011). Groundwater recharge mainly occurs twice a year, during spring (late March to early April) and late autumn (November to early December) from the infiltration of snowmelt and rainfall, respectively (Luoma and Okkonen 2014). Groundwater mainly flows northward into the coastal area and also towards the south–southeast into wetlands and peatlands, as well as towards the Baltic Sea in the east. The groundwater level rapidly responds to a rise in the sea level, as well as to recharge from the spring snowmelt and rainfall (Backman et al. 2007; Luoma et al. 2013; Luoma and Okkonen 2014).

**Fig. 3** Simulated groundwater levels based on data for the present (1971–2000) under a mean and b dry conditions





## Material and methods

### Description of the methods used

In this study, three intrinsic vulnerability mapping methods were applied and compared: a modified version of SINTACS, the AVI and GALDIT. SINTACS was selected because it has more options for the weight string based on the different environmental settings of the aquifer. Although Kirchner (2006) referred to parameter-rich models with too many degrees of freedom as “marionettes”, SINTACS provides weight strings including those factors associated with human activities and watercourses that are commonly found in shallow groundwater areas in Finland. However, the rating classifications of three (soil media, aquifer media and attenuation capacity of the unsaturated zone) of the seven parameters in SINTACS were modified based on the superficial deposit map of Finland to make the index more suitable for glacial aquifer deposits and deglaciation depositional environments, as mentioned in the previous section. The AVI is simpler than SINTACS, with only two parameters required for the analysis, and it was selected in order to compare with SINTACS to evaluate the effect of the number of parameters inputted on the vulnerability indices. However, neither SINTACS nor the AVI have parameters to determine contamination from seawater intrusion; thus, GALDIT was selected for the intrinsic vulnerability assessment of seawater intrusion into the coastal aquifer and compared with SINTACS and the AVI.

The SINTACS and GALDIT methods are based on the index weight rating and overlay analytical function using the ArcMap program, while the AVI method is based on the type and thickness of the aquifer media above the groundwater level. A brief description of each method is given below.

#### *SINTACS and the modified SINTACS*

The intrinsic vulnerability mapping method SINTACS (Civita and De Maio 2004) is based on the index weight rating and overlay analytical function using the ArcMap program. It is a modification of the DRASTIC method (Aller et al. 1987) with the improvement of more options for the weight rating of each parameter based on the different environmental settings of the aquifer. It is a parametric system with rating scores and weights for seven parameters: depth to the water table ( $S_o$ ), effective infiltration ( $I$ ), unsaturated zone attenuation capacity ( $N$ ), soil attenuation capacity ( $T$ ), hydrogeological characteristics of the aquifer ( $A$ ), hydraulic conductivity ( $C$ ) and topographical slope ( $S$ ). Each parameter was rated based on its characteristics and susceptibility to groundwater contamination from 1 (the lowest vulnerability) to 10 (the highest vulnerability). The definitions of these parameters are presented by Civita and De Maio (2004). In each grid cell, the assigned parameter ratings were then multiplied by the weight strings.

The weight strings corresponded to one of six hydrogeological environments, including normal impact, severe impact, drainage, karst, fissured and nitrate. Each weight string was assigned a value from 1 to 5, with the most significant factors receiving a weight of 5 and the least significant a weight of 1. The final vulnerability index in each grid cell was the sum of the scores for the seven parameters and was obtained by superposition of the seven thematic maps:

$$\text{SINTACS index} = SorSow + IrIw + NrNw + TrTw + ArAw + CrCw + SrSw \quad (1)$$

where

$r$  = rating

$w$  = weight string

The final vulnerability index score was divided into vulnerability classes (very high, high, medium, low and very low) to produce a final vulnerability SINTACS index map of aquifer area. The classification category was varied depending on the number of weight strings applied. A possible minimum value of 26 to a possible maximum value of 260 represents a relative measure of groundwater vulnerability. The higher the vulnerability index value, the more vulnerable the aquifer is to contamination. In this study, the modification was performed to SINTACS for three parameters: the unsaturated zone attenuation capacity, soil media and aquifer media. This was done by classifying the rating system based on the superficial deposit map of Finland, while the other parameters and weight strings were maintained as in the original SINTACS method. Further details of the modified SINTACS parameters are provided in section ‘Vulnerability index mapping’. The SINTACS vulnerability index map presented in this study is therefore a result of the vulnerability assessment performed using the modified SINTACS parameters.

#### *Aquifer vulnerability index (AVI)*

The aquifer vulnerability index (AVI) (Van Stempoot et al. 1993) is a method for mapping the vulnerability of groundwater based on two parameters: the thickness of each sedimentary unit above the uppermost saturated aquifer ( $d$ , length) and the estimated hydraulic conductivity ( $K$ , length/time) of each of these layers (Van Stempoot et al. 1993). The index is determined from the relationship between these two parameters, as shown in the following equation:

$$\text{AVI} = \sum di/Ki \text{ for layer } i \text{ to } i. \quad (2)$$

The AVI has a dimension of time and represents the hydraulic resistance of an aquifer to vertical flow. Based on these hydraulic resistances, the AVI is divided into five classes: extremely low, low, moderate, high and extremely high vulnerability, as shown in Table 1 (Van Stempoot et al. 1993). In

**Table 1** Hydraulic resistance values and corresponding vulnerability classes (Van Stempvoort et al. 1993)

Hydraulic resistance (year)	Vulnerability (AVI)
0–10	Extremely high
10–100	High
100–1,000	Moderate
1,000–10,000	Low
>10,000	Extremely low

many studies, however, the AVI classification has been modified with different criteria to suit the study area.

### GALDIT

GALDIT is an intrinsic vulnerability assessment method for assessing the vulnerability of a coastal aquifer to seawater intrusion (Chachadi and Lobo-Ferreira 2001, 2007; Chachadi et al. 2003). It was originally developed to assess the vulnerability of coastal aquifer systems to seawater intrusion in India. Similarly to SINTACS, it is a parametric system with rating scores and weights for six parameters that describe the most important factors controlling seawater intrusion: groundwater occurrence ( $G$ ), aquifer hydraulic conductivity ( $A$ ), the groundwater level above sea level ( $L$ ), distance from the shore ( $D$ ), the impact of the existing status of seawater intrusion ( $I$ ) and the thickness of the aquifer ( $T$ ). Each parameter was rated based on its characteristics and susceptibility to seawater intrusion, the alternative scores being 2.5 (lowest vulnerability) 5, 7.5 and 10 (highest vulnerability). In each grid cell, these assigned rating parameters were then multiplied by the weight strings. The weight strings were assigned a value from 1 (the least significant factor) to 4 (the most significant factor). The final vulnerability index in each grid cell was the sum of the scores of these six parameters:

$$\text{GALDIT index} = \frac{\sum_{i=1}^6 W_i R_i}{\sum_{i=1}^6 W_i} \quad (3)$$

where  $R$  is the rating and  $W$  is the weight string. The final GALDIT vulnerability index score varies from 2.5 to 10 and is divided into three vulnerability classes: high (>7.5), moderate (5 to 7.5) and low vulnerability (<5). The higher the vulnerability index value, the more vulnerable an aquifer is to seawater intrusion.

### Vulnerability index mapping

The groundwater intrinsic vulnerability assessment was performed according to the following steps:

*Step 1.* The aquifer area was defined from the saturated permeable glacial and deglacial sediments (e.g. gravel, sand and fine sand) thicker than 2 m or deposits deeper than 5 m if there was no observation of the saturated zone thickness.

*Step 2.* The intrinsic vulnerability assessments of the aquifer were performed under mean and dry (summer) climate conditions at present (1971–2000) utilizing the modified SINTACS, AVI and GALDIT methods.

*Step 3.* With the afore-mentioned methods, the intrinsic vulnerability assessment was performed under mean and dry climate conditions for the A1B (2021–2050) future climate scenario (Luoma and Okkonen 2014). The results of the vulnerability indices were compared with the present conditions.

Mapping of the groundwater intrinsic vulnerability index was performed using the ArcMap program version 10.1. Each parameter was converted to a grid map with grid cell size of  $10 \times 10$  m, covering approximately 52 km<sup>2</sup>.

The results of the climate change impact study by Luoma and Okkonen (2014), including groundwater recharge, depth to the groundwater and sea-level rise data, were used to assess the impact of climate variability and change on aquifer vulnerability. The sustainable use of groundwater should also consider the possible effects of climate change on groundwater, and this study thus provides information on whether the variability and change in the climate play a role in aquifer vulnerability assessment. Among the key parameters in vulnerability assessment are recharge and depth to the groundwater level, both affected by dynamic parameters such as precipitation, temperature and sea level. IPCC (2007) provides information on possible changes in precipitation and temperature that are rarely used in aquifer vulnerability mapping. The results for the present conditions (1971–2000) were compared with those for climate change scenario A1B during the period 2021–2050.

The rating and weighting was performed for each parameter using the map overlay analytical function in the Spatial Analyst module of the ArcMap program. The final vulnerability map was a compilation of these maps, where each cell in the grid model is represented by a vulnerability value that corresponds to the cumulative rating and weighting of all the parameters. The final vulnerability index maps were then divided into classes and the percentage of grid cells in different vulnerability classes was calculated and compared.

In addition, sensitivity analysis was performed using groundwater recharge and sea-level variability, which have the greatest impact on the groundwater level (Luoma and Okkonen 2014) and thus on the depth to the groundwater level, the thickness of the unsaturated/saturated zone and consequently the vulnerability of the aquifer.

*Modified SINTACS method*

The calculation of the modified SINTACS vulnerability index is summarized in detail below:

$$\text{SINTACS index} = So r So_w + Ir I_w + Nr * N_w + Tr * T_w + Ar * A_w + Cr C_w + Sr S_w \tag{4}$$

where

- r* is the rating for each parameter
- w* is the weight associated with each parameter in each weight string, and
- So, I, N, T, A, C* and *S* are seven parameters of the SINTACS vulnerability index and \* indicates the parameters that have been modified:

*Depth to water (So):* The depth to water parameter is the distance from the ground surface to groundwater level of the uppermost aquifer. The deeper the water table, the longer it will take for contaminants to reach the saturated zone, allowing more time for natural attenuation and lowering of the vulnerability (Aller et al. 1987). A grid map of the groundwater level was produced from the interpolation of groundwater levels from 240 observation wells distributed throughout the study area using the kriging interpolation method in ArcMap. The depth to water grid map was produced by subtracting the topographic and groundwater level grid maps. The average depth to water grid map during the period 1971–2000 ranges between 0 and 15 m, with an average value of 4 m. The vulnerability rating for the depth to water parameter is presented in Table 2.

*Recharge (I):* Groundwater recharge is an important process that can transport contaminants into the subsurface and towards the water table. In this study, groundwater recharge was obtained from the simulation of the UZF1-MODFLOW 2005 groundwater flow model with mean annual groundwater recharge during the period 1971–2000 of 283 mm (42 % of precipitation; Luoma and Okkonen 2014). The vulnerability ratings of recharge used are provided in Table 2.

*Unsaturated zone attenuation capacity (N\*):* The unsaturated zone material was identified from the uppermost texture of the soil in survey data from Finland at the scale 1:20,000 (Ahoenon et al. 2015). The attenuation capacity of the unsaturated zone was rated based on the permeability of the aquifer materials. The more permeable the material, the shorter the transit time and lower the attenuation capacity, and hence the more vulnerable the aquifer is (Aller et al. 1987). The vulnerability ratings used for the unsaturated zone attenuation capacity are presented in Table 2.

**Table 2** SINTACS parameters and ratings. Modified parameters are indicated by \*

Rating	<i>So</i>	<i>I</i>	<i>N*</i>	<i>T*</i>	<i>A*</i>	<i>C</i>	<i>S</i>
	Depth to water (m)	Recharge (mm year <sup>-1</sup> )	Unsaturated zone attenuation capacity	Soil media	Aquifer media	Hydraulic conductivity, K-values (m day <sup>-1</sup> )	Topography (slope, %)
1	>40	0–24	Confining layer, clay	Clay	Clay	<0.0043	26–30
2	24–40	25–42	Silt, silty/sandy/gravelly clay	Silty/sandy/gravelly clay	Silt, silty/sandy/gravelly clay	0.0043–0.043	22–25
3	16–24	43–66	Silt and clay	Clay loam	Gytja	0.043–0.17	19–21
4	12–16	66–92	Fine-grained till	Silt, silty loam	Fine-grained till	0.17–0.61	18–16
5	8–12	93–110	Sandy, gravelly till	Loam	Sandy, gravelly till	0.61–2.59	13–15
6	6–8	111–135	Finer fine sand	Sandy loam	Finer fine sand	2.59–6.48	10–12
7	4–6	136–162	Coarser fine sand	Aggregated clay, loamy sand	Coarser fine sand	6.48–23.33	7–9
8	3–4	163–194	Sand and gravel	Peat	Sand	23.33–62.21	5–6
9	1.5–3	195–235	Gravel	Sand	Sand and gravel	62.21–345	3–4
10	<1.5	>235	No vadose zone	Thin or absent; gravel	Gravel	>345	0–2
Weight string	<i>So</i>	<i>I</i>	<i>N</i>	<i>T</i>	<i>A</i>	<i>C</i>	<i>S</i>
Normal	5	4	5	3	3	3	3
Severe	5	5	4	5	3	2	2
Drainage	4	4	4	2	5	5	2



*Soil media (T\*)*: The thickness and texture of the soil can influence the natural attenuation capacity and permeability of the soil zone. Unfractured clays and silts provide a barrier to flow and have a lower vulnerability than more permeable sands (Aller et al. 1987). The soil material was based on soil survey data from Finland at the scale 1:20,000 (Ahonen et al. 2015). The vulnerability rating was based on the soil texture as shown in Table 2. In Hanko, the soil layer is absent in most of the aquifer area and causes the highest vulnerability in these parts.

*Aquifer media (A\*)*: Highly porous media result in high aquifer vulnerability because of the lower natural attenuation capacity of more permeable aquifers (Aller et al. 1987). Some aquifer media described in DRASTIC and SINTACS do not exist in the shallow aquifers in Finland. Hence, the aquifer media rating used in this study was based on the superficial deposit map of Finland (Ahonen et al. 2015), which displays deposits from glaciation. The aquifer media data were obtained from drilled wells and the superficial deposit map of Finland at the scale 1:20,000 (Ahonen et al. 2015), according to which approximately 80 % of the area of the Hanko aquifer consists of sand and gravel. The vulnerability ratings used for the aquifer media are presented in Table 2.

*Hydraulic conductivity (C)*: The higher the hydraulic conductivity ( $K$ -value) of an aquifer, the faster water and contaminants are able to move from the source to the groundwater, and hence the higher is the vulnerability of the aquifer (Aller et al. 1987).  $K$ -values were obtained from various data sets, including well testing, slug testing, grain-size analysis and soil analysis. The final data were obtained from the calibration of groundwater flow modelling, with the average  $K$ -values varying from 0.22 to 30 m day<sup>-1</sup>. The vulnerability ratings for different  $K$ -values are presented in Table 2.

*Topography (S)*: The vulnerability due to topography was assessed based on the percentage slope of the land surface. The greater the slope, the more potential there is for runoff and the less potential for infiltration of contaminants, and vulnerability is consequently lower (Aller et al. 1987). The LiDAR elevation model was used to calculate the slope of the topography in the Hanko area by using ArcMap with the Spatial Analyst tool. The topography in the Hanko area is generally quite flat, with the average percentage of slope being 2.5 %. The vulnerability ratings used for topography are provided in Table 2.

*Weight string of all hydrogeological zones*: A weight was assigned to each parameter in each grid cell. Three weight strings were used directly from the SINTACS weight strings (Civita and De Maio 2004), including normal impact, severe impact and drainage (Table 2). Normal impact represents an area that has no impact from human activities, while severe impact represents areas strongly

affected by human activities, and drainage represents areas that contain water bodies, such as the drainage system from streams, lakes, and in the Hanko area, the Baltic Sea coastline. The Hanko area experienced the highest sea level since 1887 at +1.24 m a.s.l. during a storm surge on 9 January 2005. The drainage area along the coastline comprised the areas that have elevation lower than 1.24 m a.s.l.

#### *Aquifer vulnerability index (AVI)*

The assessment of aquifer vulnerability using the AVI method was based on the type and thickness of aquifer media above the groundwater level. The data needed for AVI analysis consist of the following: (1) information on each hydrostratigraphic unit such as an aquifer (sand, gravel) and aquitard (clay, silt, till), (2) the hydraulic conductivity ( $K$ -value) distribution for each hydrostratigraphic unit and (3) the groundwater level distribution of the aquifer. As in the SINTACS method, the hydrostratigraphic data were obtained from a 3D geological model and groundwater flow model of the study area (Luoma and Okkonen 2014; Luoma et al. 2013).  $K$ -values were derived from well testing, slug testing, grain-size analysis, laboratory analysis and calibration of the groundwater flow model.

#### *GALDIT index*

The vulnerability rating and weight string of parameters used in GALDIT are presented in Table 3. The ratio of Cl/(HCO<sub>3</sub>+CO<sub>2</sub>) was originally recommended for rating the impact status of the existing seawater intrusion parameter by Chachadi and Lobo-Ferreira (2001). Later, Dörfliger et al. (2011) added electrical conductivity (EC) values and chloride (Cl) concentrations in groundwater from wells along the coastline as alternative indicators of existing seawater intrusion, with the rating classification based on the drinking-water standard of EC < 2,500 μS cm<sup>-1</sup> and Cl < 250 mg L<sup>-1</sup> (WHO 2011; Council of EU 1998; STM 2001). In this study, the Cl concentrations in groundwater were categorized into <50, 50–100, 100–200, and >200 mg L<sup>-1</sup> and assigned the respective ratings of 2.5, 5, 7.5 and 10. Mäkinen (2008) reported that based on the taste and the characteristics that induce corrosion, the Cl concentration in groundwater should be <25 mg L<sup>-1</sup> in order to prevent the corrosion of pipeline materials. In addition, the Ministry of Social Affairs and Health (STM 2001) recommended the concentration of Cl in drinking water to be <100 mg L<sup>-1</sup> for an acceptable taste for people; thus, in this study, a Cl concentration in groundwater of 25 mg L<sup>-1</sup> (instead of 50 mg L<sup>-1</sup>) was used as the minimum threshold of the rating classification (Table 3).

**Table 3** GALDIT parameters and ratings

Rating	Groundwater occurrence (aquifer type)	Aquifer hydraulic conductivity (m day <sup>-1</sup> )	Height of groundwater level above sea level (m)	Distance from the shore (m)	Impact status of existing seawater intrusion			Aquifer thickness (saturated) (m)
					Cl <sup>-</sup> /[HCO <sub>3</sub> <sup>-</sup> + CO <sub>3</sub> <sup>2-</sup> ] <sup>a</sup>	EC (μS cm <sup>-1</sup> )	Cl (mg L <sup>-1</sup> )	
10	Confined aquifer	>40	<1	<500	>2	>1,000	>200	>10
7.5	Unconfined aquifer	10–40	1–1.5	500–700	1.5–2	800–1,000	100–200	7.5–10
5	Leaky confined aquifer	5–10	1.5–2	700–1,000	1–1.5	400–800	25–100	5–7.5
2.5	Bounded aquifer <sup>b</sup>	<5	>2	>1,000	<1	<400	<25	<5
Weight	1	3	4	4	1	1	1	2

<sup>a</sup> In mill-equivalent per million in groundwater

<sup>b</sup> Recharge and/or impervious boundary, aligned parallel to the coast

### Vulnerability index maps: validation efforts

The vulnerability assessments were evaluated in order to verify the validation of the methods (National Research Council 1993). In this study, the predicted levels of vulnerability were compared with the results of a hydrogeochemical study by Luoma et al. (2015), which included the analysis of water samples from 15 sites and monitoring data from 15 observation wells (depth and temperature for inland observation wells, and depth, temperature and electrical conductivity (EC) for wells located along the coastline) during the years 2009–2010 and 2012. The contribution of seawater to the aquifer was calculated based on the chloride (Cl) concentrations of groundwater, seawater and freshwater using the following equation (Appelo and Postma 2005):

$$\text{Seawater fraction}(\%) = \frac{Cl_s - Cl_f}{Cl_{sw} - Cl_f} \times 100 \quad (5)$$

where  $Cl_s$ ,  $Cl_f$  and  $Cl_{sw}$  are the Cl concentrations of groundwater, local freshwater and seawater, respectively. A simplified intrusion zone was determined from the difference in the densities between the interface zone of groundwater and seawater using the Ghyben-Herzberg equation (Ghyben 1889; Herzberg 1901):

$$Z = \frac{\rho_f}{\rho_{sw} - \rho_f} h \quad (6)$$

where  $h$  is thickness of the freshwater zone above sea level,  $Z$  is the thickness of the freshwater zone below sea level,  $\rho_f$  is the density of freshwater (1.00 kg m<sup>-3</sup>) and  $\rho_{sw}$  is the density of seawater. In the Gulf of Finland, the density of seawater varies from 1.001 to 1.006 kg m<sup>-3</sup> (average 1.003 kg m<sup>-3</sup>), which is relatively low compared to normal oceanic water (average 1.025 kg m<sup>-3</sup>). The average density value of 1.003 kg m<sup>-3</sup> was used for the calculation. The length of the seawater intrusion wedge ( $L$ ) at the point beneath the shoreline into the aquifer section is expressed as (Schwartz and Zhang 2003):

$$L = 0.5 \left[ \frac{(\rho_{sw} - \rho_f)}{\rho_f} \frac{b}{dh/dx} \right] \quad (7)$$

where  $b$  is the thickness of the aquifer,  $dh$  is the thickness of the freshwater zone above sea level, and  $dx$  is the distance of well from the shoreline.

### Vulnerability analysis under climate scenarios

Climate scenarios A1B and B1 in Hanko predicted an increase in the mean temperature of at least 1.0 °C for all periods compared with the present (1971–2000) (Luoma and Okkonen 2014). Scenario A1B (2071–2100) predicted the greatest increase in the mean temperature range (2.9–4.6 °C), with an annual mean increase of 3.4 °C compared with the present. Scenario B1 (2071–2100) resulted in a similar mean temperature pattern to A1B (2071–2100), but with an approx. 1.0 °C lower mean temperature than A1B (2071–2100). For the period 2021–2050, the mean temperature in both the A1B and B1 scenarios was similar, with an annual mean increase of 1.3–1.4 °C from the present. Overall, annual precipitation in the scenarios increased by 5–12 % compared with the present, and was lowest in B1 (2021–2050) and highest in A1B (2071–2100). The average sea level in Hanko was predicted to be at +0.09 m in the B1 scenario (medium regionalised) and +0.51 m in the A1B scenario (highly regionalised) by the end of the 21st century.

However, the highest increase in groundwater recharge (with an average increase of 33 % from the present) and the groundwater level in Hanko (with an average increase of 0.98 m from the present) was predicted from the flow simulation utilising the climate and sea level rise scenario A1B (2021–2050) (with the predicted sea level at +0.13 m). Moreover, the groundwater level fluctuation pattern in Hanko shows clear seasonal variations, where the maximum groundwater level occurs during spring immediately

after snowmelt and the minimum groundwater level occurs during the summer due to high evapotranspiration and low precipitation (Luoma and Okkonen 2014). For the selected vulnerability assessment methods (modified SINTACS, AVI and GALDIT), climate change will have impacts on the parameters that are relevant to the groundwater level (groundwater recharge, depth to water, height of groundwater level above sea level and thickness of the saturated zone). Hence, groundwater vulnerability under a climate change scenario was assessed based on the groundwater level data obtained from A1B (2021–2050) under mean and dry climate conditions. The other parameters (unsaturated zone material, soil media, aquifer media,  $K$ -value and slope) were assumed to remain static, as under the present conditions. The vulnerability index maps under climate scenario A1B (2021–2050) were compared with the vulnerability index for the present. For more detailed information on the impacts of climate change on groundwater recharge and surface leakage in Hanko, the reader is referred to the study of Luoma and Okkonen (2014).

### Sensitivity analysis

Sensitivity analysis was performed to examine the contribution of single parameters to the vulnerability index map. Because groundwater recharge and sea-level rise have direct impacts on the groundwater level and surface leakage (as mentioned previously) in Hanko, these two parameters were selected for the sensitivity analysis by arbitrarily changing the values of both parameters by certain percentages from the initial condition. Groundwater recharge was changed by 10, 20 or 30 % from the present (mean) condition, while the sea level remained unchanged, and vice versa. The vulnerability index was calculated based on the results of the simulations and compared with the vulnerability index for the initial condition. The effect of changing the specific parameters was calculated using the following equation (Li and Merchant 2013):

$$V\% = \frac{V_x - V_i}{V_i} \times 100 \quad (8)$$

where  $V\%$  is the variation in the groundwater vulnerability index expressed as a percentage,  $V_x$  is the vulnerability score affected by changes in specific parameter  $x$ , and  $V_i$  the vulnerability score for the initial condition. For the modified SINTACS and GALDIT, changes in the areas classified as having high and extremely high vulnerability were determined for each change of the parameter and compared with the initial condition. For the AVI, the change in the area having ‘hydraulic resistance within 2 days’ was calculated and compared with the initial condition.

## Results

### Vulnerability index maps of Hanko

Figure 4 displays rating and weight string maps for the modified SINTACS parameters and Fig. 5a the final SINTACS intrinsic vulnerability index map of the Hanko aquifer at present (1971–2000). The SINTACS vulnerability scores for the Hanko aquifer range from 112 to 248, which are classified as medium to extremely high vulnerability, where 99 % of the total area has high to extremely high vulnerability. The area of extremely high vulnerability (77 % of the total area) is located in the low-lying area in central-northern and northeastern parts of Hanko.

The hydraulic resistances of the Hanko aquifer at present, calculated using the AVI method (Fig. 5c), vary between less than a day to 47 days. Based on the AVI vulnerability index classification from Van Stempvoort et al. (1993), all of the Hanko aquifer is classified as extremely high vulnerability. For comparison with SINTACS, the AVI hydraulic resistance map was divided into four classes using the geometric classification in the Spatial Analyst module.

Figure 6 displays the GALDIT vulnerability index map of the Hanko aquifer at present (1971–2000) under (1) mean and (2) dry (summer) climate conditions. The GALDIT vulnerability index map was classified into low, moderate and high vulnerability, with 5.7 % (~2.6 km<sup>2</sup>) and 10.7 % (~4.9 km<sup>2</sup>) of total area classified as high vulnerability under the present mean and dry climate conditions, respectively.

### Vulnerability index maps under climate change scenarios

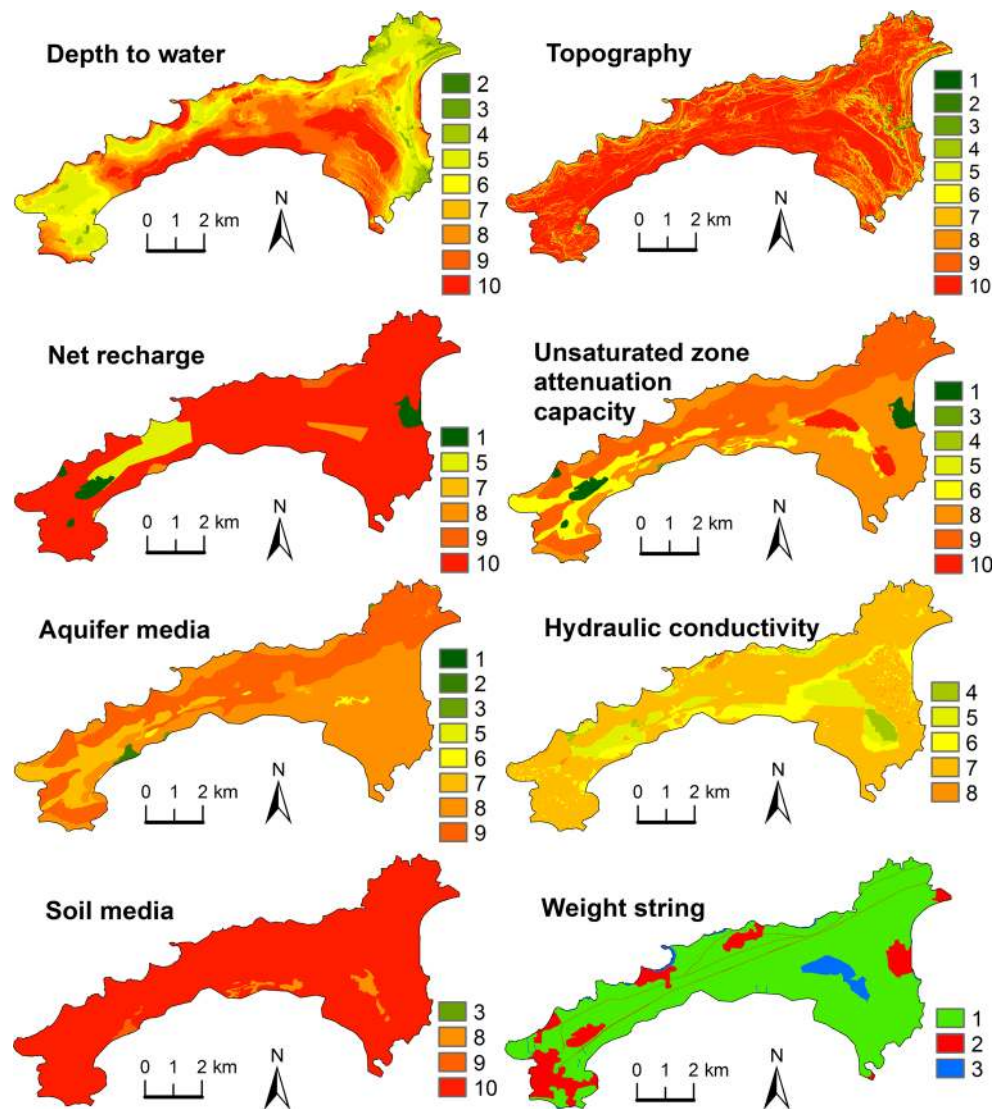
The SINTACS intrinsic vulnerability index map of Hanko aquifer under climate scenario A1B (2021–2050; Fig. 5b) contains vulnerability scores ranging from 112 to 292, which were classified as medium and extremely high vulnerability. The area classified as having extremely high vulnerability was 1.75 km<sup>2</sup> (3.79 % of the total aquifer area) greater than at present.

For the AVI, the hydraulic resistances under the A1B scenario (2021–2050) were found to vary from less than a day to 42 days and had a similar distribution pattern as at present. However, the hydraulic resistance values were 1.0–5.0 days lower compared to the present (Fig. 5d).

The GALDIT vulnerability index maps of the Hanko aquifer under present conditions and scenario A1B (2021–2050) for both mean and dry season conditions are presented in Fig. 6. The map area with a high GALDIT vulnerability index covers 4.8 km<sup>2</sup> (10.7 % of total), 4.2 km<sup>2</sup> (9.3 %), 2.6 km<sup>2</sup> (5.7 %) and 1.8 km<sup>2</sup> (3.9 %), respectively, for data from the present in the dry season, A1B (2021–2050) in the dry season, the present under mean conditions and A1B (2021–2050) under mean conditions. Under dry climate conditions, both at



**Fig. 4** Rating grid maps of the modified SINTACS parameters and weight string based on data for the present (1971–2000)



present and under the A1B scenario (2021–2050), the aquifer area with high groundwater vulnerability to seawater intrusion also included the aquifer in the inland areas in the western part of the study area, near to the town of Hanko, which has low groundwater levels and a relatively low hydraulic gradient compared to the sea level.

#### Vulnerability index maps: validation efforts

According to the results from the AVI and the modified SINTACS method, the Hanko aquifer is classified as having high to extremely high vulnerability. The integration of multivariate statistical approaches (principal component analysis (PCA) and hierarchical cluster analysis (HCA)) with conventional classification of groundwater types), as well as with the hydrogeochemical data from Luoma et al. (2015), identified the vulnerable groundwater areas based on the impacts of both natural and human activities on water quality. The natural

impacts on groundwater vulnerability were observed in most parts of the aquifer area, which are still uncontaminated. This is indicated by the low dissolved element concentrations, low pH and alkalinity due to rapid percolation or a short residence time. The stable isotopes  $\delta^2\text{H}$  and  $\delta^{18}\text{O}$  also clearly suggest that the Hanko aquifer recharges directly from meteoric water.

The impacts of human activities on groundwater vulnerability were localised in areas near human activities and can be observed, for example, from the continued increase in  $\text{NO}_3$  and metal concentrations in groundwater, or the high Na and Cl concentrations in groundwater due to the impact of the de-icing road salt. Moreover, the geochemistry of groundwater in the Hanko aquifer varies spatially and temporally according to changes in the hydrological conditions, such as precipitation events and snowmelt. These indicate a highly vulnerable aquifer with high susceptibility to water from the ground surface percolating down to the water table, which corresponds well to the results of the AVI and modified SINTACS.

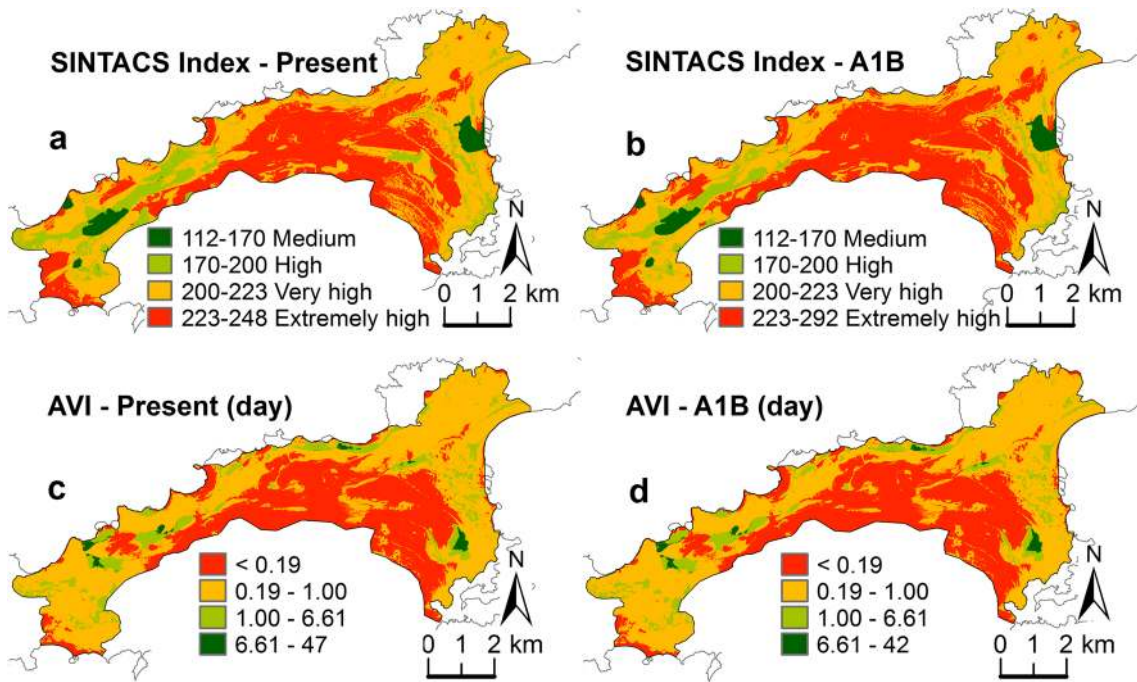


**Fig. 5** SINTACS intrinsic vulnerability index map based on data for the present (1971–2000) (a) and under future climate scenario A1B (2021–2050) (b). The distribution of hydraulic resistances (days) calculated with

the AVI with data for the present (1971–2000) (c) and under climate scenario A1B (2021–2050) (d)

Regarding the influence of seawater intrusion, the Cl concentration of seawater in the Hanko area was  $2,690 \text{ mg L}^{-1}$ , while the Cl concentrations of groundwater from wells along the coastline (Obs10 and Obs11) varied between 5.10 and  $8.60 \text{ mg L}^{-1}$ . EC values of seawater varied between  $7,510$  and  $10,300 \text{ }\mu\text{S cm}^{-1}$ , and those of groundwater from Obs10,

Obs11 and Obs14 varied between  $163$  and  $380 \text{ }\mu\text{S cm}^{-1}$ . Based on Eq. (5) and the chloride concentration of local freshwater of  $1.10 \text{ mg L}^{-1}$ , the calculated contributions of seawater to the aquifer were approximately 0.15–0.28 %. Based on Eqs. (6) and (7), the thickness of the freshwater zone below sea level ( $Z$ ) and the length of the seawater intrusion wedge

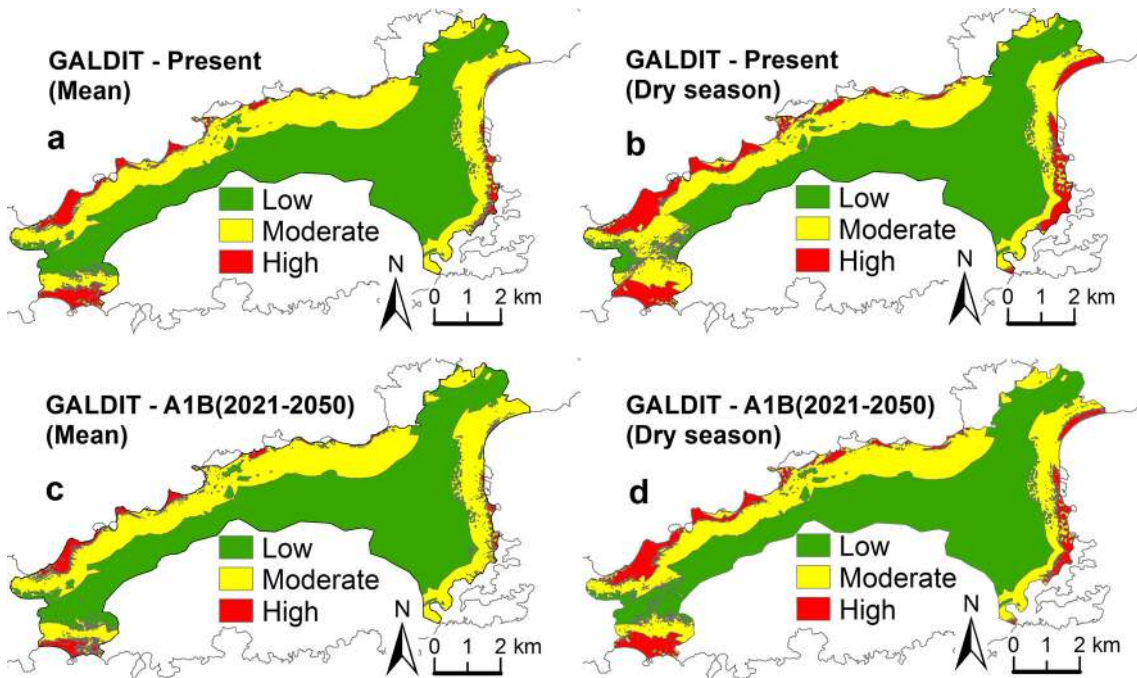


**Fig. 6** GALDIT vulnerability index maps based on data for the present (1971–2000) under a mean and b dry conditions, and climate scenario A1B (2021–2050) under c mean and d dry conditions

( $L$ ) from the point beneath the shoreline into the aquifer section at three observation wells (Obs10, Obs11 and Obs14; Fig. 1) during the highest EC values of the measurements were in the ranges 186.7–716.7 and 4.3–12.5 m for the  $Z$  and  $L$  values, respectively (Table 4). The  $Z$  thicknesses were approximately 9–21 times thicker than the thickness of the aquifer, which indicates the thickness of the freshwater zone covering all of the aquifer section, which agrees well with the geochemical and monitoring results indicating a small contribution of seawater to the aquifer. However, these three wells are located in the GALDIT high vulnerability index map areas; nevertheless, the geochemistry of groundwater from Obs10, which is located near the coastline and the water intake well, suggests sulphate reduction in the mixed zone between fresh and seawater, indicating that local seawater intrusion may temporarily take place in this area due to the intrusion of seawater either from sea-level rise or the influence of groundwater pumping (Luoma et al. 2015).

### Sensitivity analysis

The results of sensitivity analysis are summarised in Table 5. For reference, the groundwater levels of wells on the coastline (Obs10) and inland (Obs1; Fig. 1) measured for each parameter changed are also presented. The initial condition is referred to as the present (mean) condition.

## Discussion

### Vulnerability index map of Hanko

According to the results based on the AVI and modified SINTACS, the Hanko aquifer is classified as highly to extremely highly vulnerable. Although the AVI indicates a higher vulnerability than the modified SINTACS, the distribution pattern of aquifer vulnerability based on the AVI is similar to that of the modified SINTACS. Both methods show extremely high vulnerability in the low-lying areas, including the areas along the shoreline and most parts of the aquifer in Santala in central-northern and northeastern parts of Hanko

(including the gravel excavation pit area) (Fig. 1). These areas consist of permeable aquifer media (gravel and sand), and the groundwater level is close to soil surface and rapidly responds to precipitation during the snowmelt period and heavy rainfall events (Luoma et al. 2015).

The purpose of the AVI is to reduce the redundant parameters used in SINTACS. It ignores the topography, because it regards this as a non-critical parameter, and also climate data such as groundwater recharge, because such data are often difficult to obtain. According to Van Stempoot et al. (1993), the influence of these parameters can be identified during later detailed site investigation in aquifer areas that are classified as highly vulnerable. These parameters are important and can be critical for assessing the intrinsic vulnerability of groundwater, e.g. in the topographic landforms of shallow aquifers that are highly variable following the depositional processes during glaciations and deglaciations. In Hanko, the case study site, the topographic landform is relatively flat, which creates low surface runoff and provides more time for precipitation to infiltrate into the aquifer.

The depth from the ground surface to the water table is one of the most important parameters in vulnerability assessment (Aller et al. 1987). Under climate change scenarios, e.g. A1B (2021–2050), an increase in groundwater recharge and the groundwater level in the future will reduce the depth to the groundwater and cause the aquifer to become more vulnerable than under present climate conditions. Nevertheless, the AVI has no parameter to determine the vulnerability of an aquifer to seawater intrusion, while SINTACS has the option of a seepage/drainage weight string for aquifers that are connected to a watercourse; however, the seepage/drainage weight string only determines the vulnerability of aquifer areas vertically from the ground surface to groundwater level, and not along a lateral interface relative to seawater intrusion. For this reason, the GALDIT index map, which takes into account the height of the groundwater level relative to the sea level, the distance of the aquifer from the shoreline and evidence of seawater intrusion, may provide a better insight into the vulnerability of an aquifer to seawater intrusion than the SINTACS and AVI methods. The results of this study indicate that GALDIT could be used in combination with the other

**Table 4** Parameters used for the calculation of the thickness of the freshwater zone below sea level ( $Z$ ) and the length of the seawater intrusion wedge ( $L$ ) from the point beneath the shoreline into the aquifer section at three observation wells (Obs10, Obs11 and Obs14) based on Eqs. (6) and (7)

Well	Date of measurement	EC ( $\mu\text{S cm}^{-1}$ )	GW level, $h$ (m a.s.l.)	Sea level (m)	$Z$ (m)	$x$ (m)	$b$ (m)	$dh/dx$	$L$ (m)
Obs10	4.10.2009	170.7	0.59	0.47	186.7	50	20	0.0024	12.5
Obs11	4.10.2009	320.8	0.75	0.47	250.0	100	20	0.0028	10.7
Obs14	4.10.2009	342.0	2.15	0.47	716.7	180	34	0.0093	5.5
Obs14	20.2.2010	380.0	1.64	-0.52	546.7	180	34	0.0120	4.3

$h$  groundwater (GW) level above sea level,  $Z$  thickness of the freshwater zone below sea level,  $x$  distance of well from the shoreline,  $b$  thickness of the aquifer,  $dh/dx$  hydraulic gradient between two measuring points,  $L$  length of the seawater intrusion wedge at the point beneath the shoreline into the aquifer section



**Table 5** Results of sensitivity analysis

Model input parameter	Change in parameter (% increase)	Increase in groundwater level (m)		SINTACS: extremely high vulnerability		AVI: hydraulic resistance of 2 days		GALDIT: high vulnerability	
		Obs10 (coastal)	Obs1 (inland)	%	km <sup>2</sup>	%	km <sup>2</sup>	%	km <sup>2</sup>
Initial condition	None	0.07 m a.s.l.	12.63 m a.s.l.	–	32.97	–	45.24	–	2.59
Recharge	10	0.05	0.37	2.47	1.14	0.68	0.39	–0.41	–0.17
	20	0.10	1.41	3.01	1.60	1.20	0.69	–0.62	–0.28
	30	0.15	2.06	3.50	5.25	2.80	1.29	–1.31	–0.59
Sea level rise	10	0.09	0.02	0.22	0.10	0.03	0.02	0.01	0.003
	20	0.19	0.05	0.29	0.13	0.06	0.04	0.23	0.10
	30	0.29	0.08	0.36	0.17	0.10	0.06	0.46	0.21
	50	0.48	0.13	0.49	0.22	0.16	0.09	1.95	0.88

A *negative value* indicates a smaller value than the initial condition

methods (e.g. SINTACS and the AVI) in assessing the intrinsic vulnerability of groundwater in coastal aquifers.

The modified SINTACS presented in this study could be applied and developed to the same standard of groundwater vulnerability assessment for inland aquifers, such as the shallow groundwater areas in Finland or elsewhere, that have similar depositional environments. The AVI classified the Hanko aquifer as high to extremely high vulnerability, especially based on the original AVI classification system (Van Stempoot et al. 1993). The classification criteria of the groundwater intrinsic vulnerability index for the AVI could possibly be improved to make the index better suited to this type of depositional environment.

### Vulnerability index maps: validation and assessment methods

Although groundwater vulnerability assessments have been reported in many study areas around the world, few studies have reported the validation of the methods used. In these, the hydrogeochemistry of groundwater samples has commonly been applied to validate aquifer vulnerability index maps. Allouche et al. (2015) applied the concentrations of contaminant indicators, e.g. NO<sub>3</sub> and Cl, for inland and coastal aquifers, but provided no concrete conclusion on the validity of the methods. Trabelsi et al. (2016) compared the GALDIT vulnerability index maps with the distribution of indicators for seawater intrusion such as TDS, Cl and the Na/Cl ratio, and the integration multiple approaches, including the extent of the freshwater–seawater interface from the Ghyben-Herzberg model. According to the results, the extent of seawater intrusion based on the Ghyben-Herzberg model corresponded well with the GALDIT medium and high vulnerability index, while the hydrogeochemical data showed poor agreement with the GALDIT index map. The areas with high concentrations of TDS and Cl but a low GALDIT vulnerability index were

interpreted to be a result of water quality deterioration rather than seawater intrusion.

The validation of the methods used for vulnerability assessment was not an easy task in the Hanko case study area, where the aquifer is vulnerable to climate change and human activities and still remains uncontaminated in many parts of the aquifer area. This can be an unsuitable situation to use the concentrations of indicators of contamination, e.g. NO<sub>3</sub>, Cl, for the validation of the assessment methods. Instead, the integration of multivariate statistical approaches with hydrogeochemical data (Luoma et al. 2015) provided useful tools to classify the vulnerable groundwater areas representing the impacts of both natural and human activities on water quality. The vulnerability index maps based on the AVI and SINTACS were consistent with the geochemical data. On the other hand, the GALDIT vulnerability index maps showed poor agreement with the contribution of seawater, and the extent of the saltwater and freshwater interface from the Ghyben-Herzberg model; however, the hydrogeochemistry of the groundwater in Hanko indicated temporal and spatial variations and suggested the temporal intrusion of seawater into the low-lying coastal aquifer area near the pumping well. The seasonal variations in groundwater discharge and overpumping could induce more seawater to enter the aquifer, but this could not be detected from the small number of water samples taken during short sampling periods. In addition, in the brackish seawater environment, where the density and salinity of seawater are much lower than oceanic water, the validity of the rate and weight strings in GALDIT, e.g. the distance from the seashore, might possibly be modified.

### Sensitivity analysis

The sensitivity analyses (Table 5) revealed that changes in groundwater recharge cause the greatest changes in the simulated groundwater level and vulnerability index compared

with sea-level rise. This indicates that groundwater recharge has a larger contribution to the variation in the groundwater level, depth to the groundwater and, consequently, groundwater vulnerability across the study area.

As groundwater recharge increases, the vulnerability indices based on SINTACS and AVI also increase, but the rate of increase in the SINTACS index is higher than that of the AVI. Conversely, an increase in groundwater recharge causes a reduction in the GALDIT vulnerability index. In the coastal area, an increase in groundwater recharge will cause more groundwater discharge into the sea and hence a lower vulnerability to seawater intrusion, as also shown by Werner et al. (2012).

An increase in the rate of sea-level rise causes the vulnerability indices derived by the three methods to increase, but with the smaller rates of increase than the increase in groundwater recharge. A change in the sea-level rise has a less significant impact on the AVI compared to SINTACS and GALDIT.

The influence of sea-level rise on the groundwater level was observed at wells located along the coastline, in which a change in the sea level has been observed to have a direct influence on the shallow groundwater level after a short time lag (Backman et al. 2007; Luoma and Okkonen 2014), while the groundwater levels of inland wells are less impacted by a change in the sea level. This result is consistent with Werner and Simmons (2009); however, the sensitivity analysis indicated that in the Hanko area, even with a sea level rise of up to 50 %, which is close to the maximum level of sea level rise under the A1B (2071–2100, highly regionalised) scenario, the groundwater level of wells along the coastline would only increase by 0.48 m, and the vulnerability index would increase by less than 1 % in SINTACS and the AVI and less than 2 % in GALDIT.

The monitoring of EC values and the Cl concentration of seawater and groundwater indicates that the contribution of seawater to the aquifer was approximately 0.15–0.28 %. In future climate change scenarios, the salinity in the Baltic Sea region is predicted to decrease by about 2–50 % from the present level (Neumann et al. 2012; Meier et al. 2006), due to the predicted increase in freshwater inflow into the Baltic Sea. Millero and Kremling (1976) also reported that the salinity of water samples from the Baltic Sea appears to have remained stable during 30 years of water sampling. The degree of seawater intrusion into the Hanko aquifer would therefore probably remain the same, even if the sea level rises to +0.51 m by the end of the 21st century, as predicted in the A1B scenario (highly regionalised).

### Impacts of climate change and seawater intrusion on aquifer vulnerability

The shallow aquifer at Hanko is located in a cold, snow-dominated region where the groundwater level clearly

displays seasonal variation. The maximum groundwater level occurs during the spring after snowmelt and in the autumn due to the lower evapotranspiration rate. The minimum groundwater level occurs during the winter due to the lack of percolation resulting from the snow cover and during the summer due to the higher evapotranspiration rate. Under climate change scenarios, the seasonal impacts of climate change and climate variability on groundwater recharge and the groundwater level will be more significant (Luoma and Okkonen 2014; Okkonen 2011; Mäkinen et al. 2008).

These will consequently affect the groundwater vulnerability indices derived from different methods applied in different seasons during a year. As mentioned in the previous section, with an increase in groundwater recharge, such as in spring, the index of groundwater vulnerability to contamination on the ground surface based on SINTACS and the AVI will also increase, while the GALDIT index will show the opposite change.

Based on climate change scenarios, increasing precipitation can cause an increasing frequency of heavy rainfall events, which are associated with flash floods and the intrusion of surface waters into aquifers. Surface water may contain bacteria, a high amount of organic carbon and other dissolved solids, which will cause a deterioration in groundwater quality (Tarvainen et al. 2013). Luoma et al. (2015) reported high concentrations of  $\text{KM}_n\text{O}_4$  in the observation wells located next to the lake and low-lying aquifer areas in Hanko, which indicated surface water intrusion into the groundwater. Increasing temperatures will cause snowmelt to occur earlier in the year and will affect the distribution of surface runoff and lead to increasing groundwater recharge in winter. Increasing groundwater recharge will lead to a rise in the groundwater level and an increase in surface leakage, which may cause flooding in the aquifer area (Luoma and Okkonen 2014). This could also increase aquifer vulnerability by enhancing the transport of surface and soil contamination into the aquifer.

On the other hand, with a decrease in groundwater recharge, such as in the summer, the index of groundwater vulnerability to contamination from the ground surface based on SINTACS and the AVI will decrease, while the index of vulnerability to seawater intrusion based on GALDIT will increase. Because decreasing groundwater recharge will lower the groundwater level relative to the seawater level, there will be a decline in the hydraulic gradient and groundwater flow velocity, and this could reduce groundwater flux discharge to the sea and induce greater seawater intrusion into the aquifer.

In the Hanko area, sea level changes have a direct effect on shallow water tables after a short time lag (Backman et al. 2007). Seawater intrusion may occur continuously and the degree of intrusion depends on the seawater and freshwater interface mechanisms and many factors associated with natural and anthropogenic sources and human activities. Although the present contribution of seawater to the aquifer was found

to be less than 0.3 %, the hydrogeochemical data from Luoma et al. (2015) indicate the possibility of temporal seawater intrusion into the low-lying coastal area, near to the water intake well areas. Ferguson and Gleeson (2012) reported that groundwater abstraction could cause a greater increase in the vulnerability to seawater intrusion for a low-lying coastal aquifer than sea-level rise. In the Hanko area, overpumping due to the seasonal increase in the groundwater demand during the summer, for example from the increased number of tourists and/or the owners of summer cottages (Luoma et al. 2013), could lower the groundwater level, especially in the water intake area, and may cause the aquifer to become more vulnerable to seawater intrusion. Under drought conditions, this could lead to a potential water shortage during the summer.

In addition, the coastal flooding of the low-lying area due to storm surges could transport potential contaminants from seawater into the aquifer. Figure 7 presents a geological cross-section of wells along the coastline in the Santala area.  $H_0$  represents the mean sea level at present (1971–2000) and  $H_1$  represents the highest storm surge in Hanko at 1.24 m a.s.l., which occurred on 9 January 2005 and caused parts of the low-lying aquifer area, such as at Obs10, to be submerged under seawater. Based on climate change scenarios A1B and sea-level rise A1B (highly regionalised; Luoma and Okkonen 2014), the mean sea level is predicted to reach +0.51 m a.s.l. and the potential storm surges would reach 1.75 m a.s.l. ( $H_2$ ) by the end of the 21st century. At this level, the areas below +0.51 m a.s.l. would be under seawater, and the areas below 1.75 m a.s.l., including the water intake well, that are located between Obs10 and Obs11, will be vulnerable to coastal flooding.

By the end of the 21st century, the density and salinity of the Baltic Sea water are predicted to be the same or lower due to the increasing input of freshwater into the Baltic Sea (Meier

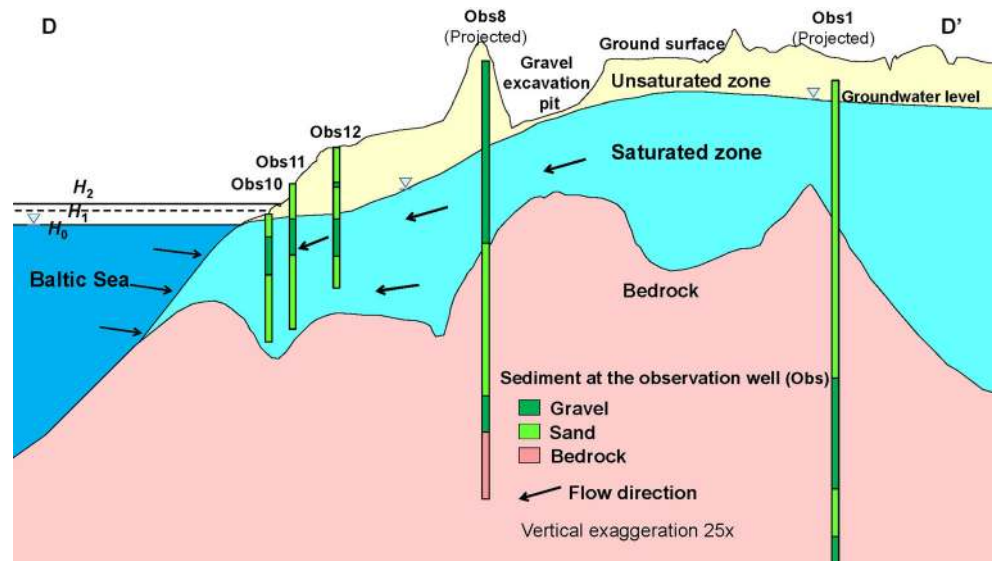
et al. 2006). The degree of seawater intrusion is therefore probably not the main concern compared with coastal flooding of the aquifer due to sea-level rise and storm surges.

Based on the main findings in this study, the degree of groundwater vulnerability to contamination and seawater intrusion of the Hanko aquifer greatly depends on climate change variability in the long term and could also vary following the seasonal variations during the year in either high or low groundwater recharge. This will challenge the management of the water supply and the strategy applied for the coastal aquifer in Hanko, including optimisation between groundwater abstraction and the intrusion rate of seawater for the water intake wells during the peak season in summer, the possibility of establishing a new water intake well further inland owing to the threats of future sea-level rise and storm surges, and the protection of groundwater to maintain water quality that meets the drinking-water standards and prevent it from contamination.

## Conclusions

Groundwater intrinsic vulnerability indices calculated using the AVI and modified SINTACS methods show high to extremely high groundwater vulnerability of the shallow unconfined low-lying aquifer in Hanko to contamination from sources on the ground surface, with the AVI indicating higher vulnerability than the modified SINTACS. The parts of the aquifer having a high vulnerability index are located in the low-lying areas consisting of permeable sediments, where the groundwater level is close to the soil surface and rapidly responds to changes in groundwater recharge. The results from the GALDIT method provide a better insight into groundwater vulnerability to seawater intrusion of the coastal

**Fig. 7** A geological cross-section along line  $D-D'$  (Fig. 1) illustrating the groundwater level and mean sea level ( $H_0$ ) at present (1971–2000).  $H_1$  represents the highest storm surge depth in Hanko at 1.24 m a.s.l. on 9 January 2005, and  $H_2$  represents the potential highest storm surges at 1.75 m a.s.l. by the end of the 21st century based on the climate change scenarios A1B and sea-level rise A1B (highly regionalised)





aquifer, particularly in areas having a low hydraulic gradient, which cannot be identified by the AVI or modified SINTACS.

The degree of groundwater vulnerability varies depending on the climate change variability and is strongly impacted by seasonal variation in groundwater recharge. Increasing groundwater recharge will increase the groundwater level and surface leakage, and will also increase the vulnerability of the groundwater to contamination from anthropogenic sources on the ground surface, as indicated by the AVI and modified SINTACS. This is the opposite result to that from GALDIT, which indicates low groundwater vulnerability to seawater intrusion due to the relatively high groundwater flux discharge to the sea. In contrast, decreasing groundwater recharge will lower the groundwater level and groundwater flooding or surface leakage may not occur, but this will increase the vulnerability of the groundwater to seawater intrusion because of the reduction in the groundwater flux discharge to the sea.

The contribution of seawater to the aquifer at present is very small. The degree of seawater intrusion in the future will probably remain the same as at present. However, overpumping could induce greater seawater intrusion into the aquifer. The sea-level rise predicted under climate change scenarios will cause some areas along the coastline to be submerged under seawater. Together with the coastal flooding of low-lying areas due to storm surges, this could potentially introduce more contamination from seawater into the aquifer.

The sensitivity analysis indicated that variation in groundwater recharge has the greatest impact on the groundwater level and consequently on groundwater vulnerability across the study area compared with sea-level rise. A change in the sea level will have an insignificant impact on groundwater vulnerability according to the AVI compared with the results based on the modified SINTACS and GALDIT. The AVI is probably not suitable for groundwater vulnerability assessment of coastal aquifers or of aquifers that are likely to be strongly impacted by climate change. The modified SINTACS could be used as a guideline for the groundwater vulnerability assessment of inland aquifers formed in glacial and deglacial deposits. Furthermore, a combination of the modified SINTACS and GALDIT could provide a useful tool to assess the vulnerability of groundwater to both contamination from sources on the ground surface and seawater intrusion for the shallow unconfined low-lying coastal aquifers under the future climate change conditions.

**Acknowledgements** This study was supported by the Groundwater Research Programme (PV3D-2263000) at the Geological Survey of Finland (GTK), and parts of the data were received from the BaltCICA Project (Climate Change: Impacts, Costs and Adaptation in the Baltic Sea Region), which was part-financed by the European Union in the Baltic Sea Region Programme 2007–2013. This manuscript was greatly improved by the reviews of Grant Ferguson, Fotis Pliakas and Sue Duncan.

**Open Access** This article is distributed under the terms of the Creative Commons Attribution 4.0 International License (<http://creativecommons.org/licenses/by/4.0/>), which permits unrestricted use, distribution, and reproduction in any medium, provided you give appropriate credit to the original author(s) and the source, provide a link to the Creative Commons license, and indicate if changes were made.

## References

- Ahonen J, Huusko A, Sallasmaa O, Palmu JP, Virkki H, Valjus T, Saarelainen J, Räisänen J, Martinkauppi A, Väänänen T, Putkinen N, Putkinen S, Huttunen T, Laxström H, Nurminen T (2015) Thickness of superficial deposits in Finland. The 2nd Finnish National Colloquium of Geosciences. Helsinki University, Helsinki
- Aller L, Bennett T, Lehr JH, Petty RH, Hackett G (1987) DRASTIC: a standardized system for evaluating groundwater pollution potential using hydrogeologic settings. USEPA report 600/2-87/035. Robert S. Kerr Environmental Research Laboratory, Ada, OK
- Allouche N, Brahim FB, Gontara M, Khanfir H, Bouri S (2015) Validation of two applied methods of groundwater vulnerability mapping: application to the coastal aquifer system of Southern Sfax (Tunisia). *AQUA* 64(6):719–737
- Appelo CA, Postma D (2005) *Geochemistry, groundwater and pollution*. Balkema, Leiden, The Netherlands
- Ataie-Ashtiani B, Werner AD, Simmons CT, Morgan LK, Lu C (2013) How important is the impact of land-surface inundation on seawater intrusion caused by sea-level rise? *Hydrogeol J* 21:1673–1677. doi:10.1007/s10040-013-1021-0
- Backman B, Luoma S, Schmidt-Thomé P, Laitinen J (2007) Potential risks for shallow groundwater aquifers in coastal areas of the Baltic Sea, a case study in the Hanko area in south Finland. CIVPRO Working Paper 2007 (2), Geological Survey of Finland, Espoo, Finland
- Barlow PM (2003) Ground water in fresh water-salt water environments of the Atlantic Coast. *US Geol Surv Circ* 1262. <http://pubs.usgs.gov/circ/2003/circ1262/pdf/circ1262.pdf>. Accessed 24 February 2012
- Beebe CR, Ferguson G, Gleeson T, Morgan LK, Werner AD (2016) Application of an analytical solution as a screening tool for Sea Water Intrusion. *Groundwater*. doi:10.1111/gwat.12411
- Chachadi AG, Lobo-Ferreira JP (2001) Seawater intrusion vulnerability mapping of aquifers using GALDIT method. Proceedings of the workshop on modelling in hydrogeology, Anna University, Chennai, India, Nov 2001
- Chachadi AG, Lobo-Ferreira JP (2007) Assessing aquifer vulnerability to seawater intrusion using GALDIT method: part 2, GALDIT indicators description. *Water Celt Countries Quant Qual Clim Var* 310:172–180
- Chachadi AG, Lobo-Ferreira JP, Noronha L, Choudri BS (2003) Assessing the impact of sea-level rise on salt water intrusion in coastal aquifers using GALDIT, APRH/CEAS. *Seminário Sobre Águas Subterrâneas*, Lisbon, Feb 2003
- Civita M (1994) *Le Carte della vulnerabilità degli acquiferi all'inquinamento: teoria & pratica* [Aquifer vulnerability to pollution maps: theory and practice]. Pitagora, Bologna, Italy
- Civita M, De Maio M (2004) Assessing and mapping ground water vulnerability to contamination: the Italian “combined” approach. *Geofis Int* 43(4):4–19
- Council of EU (1998) Council Directive 98/83/EC of 3 November 1998 on the quality of water intended for human consumption. [http://ec.europa.eu/environment/water/water-drink/legislation\\_en.html](http://ec.europa.eu/environment/water/water-drink/legislation_en.html). Accessed 24 June 2014
- Dörfliger N, Dumon A, Aunay B, Picot G, Moynot C, Bollard M (2011) Influence de la montée du niveau de la mer sur le biseau salin des aquifères côtiers des DROM/COM, Rapport final [Influence of rising sea levels on the salt wedge of coastal aquifers of the DROM/COM,

- Final report]. BRGM RP-60828-FR. BRGM, Orléans, France. [http://www.onema.fr/IMG/pdf/2011\\_047-2.pdf](http://www.onema.fr/IMG/pdf/2011_047-2.pdf). Accessed 12 June 2015
- Ferguson G, Gleeson T (2012) Vulnerability of coastal aquifers to groundwater use and climate change. *Nat Clim Chang* 2:342–345. doi:10.1038/NCLIMATE1413
- Foster SSD (1987) Fundamental concepts in aquifer vulnerability, pollution risk and protection strategy. In: van Duijvanbooden W, van Waegeningh HG (eds) Vulnerability of soil and groundwater to pollution. TNO Committee on Hydrological Research, Delft, The Netherlands
- Fyfe GJ (1991) The morphology and sedimentology of the Salpausselkä I Moraine in southwest Finland. Cambridge University, Fitzwilliam College, Cambridge
- Ghyben BW (1889) Nota in Verband met de Voorgenomen Putboring Nabij Amsterdam [Memorandum related to planned well drilling near Amsterdam]. *Tijdschr Koninkhik Inst Ing* 9:8–22
- Herzberg B (1901) Die Wasserversorgung einiger Nordseebäder [The water supply of some resorts on the North Sea]. *J Gasbeleuchtung Wasserversorg* 44:815–844
- IPCC (2000) Emissions scenarios: summary for policymakers: a special report of IPCC Working Group III. <http://www.ipcc.ch/pdf/special-reports/spm/sres-en.pdf>. Accessed 21 November 2011
- IPCC (2007) Climate Change 2007: impacts, adaptation and vulnerability: summary for policymakers. In: Contribution of Working Group II. In: Parry ML, Canziani OF, Palutikof JP, van der Linden PJ, Hanson CE (eds) The Fourth Assessment Report of the Intergovernmental Panel on Climate Change. Cambridge University Press, Cambridge, UK, pp 7–22
- Ivkovic KM, Dixon-Jain P, Marshall SK, Sundaram B, Clarke JDA, Wallace L, Werner AD (2013) A national-scale vulnerability assessment of sea-water intrusion: literature review, data review, and method development. Record 2013/03. Geoscience Australia, Canberra, and National Centre for Groundwater Research and Training, Adelaide, Australia
- Kielosto S, Kukkonen M, Sten CG, Backman B (1996) Hangon ja Perniön kartta-alueiden maaperä [Quaternary deposits in the Hangon and Perniö map-sheet areas, Geological map of Finland 1: 100,000, Explanation to the maps of Quaternary deposits, sheets 2011 and 2012]. Geological Survey of Finland, Espoo, Finland
- Kirchner JW (2006) Getting the right answers for the right reasons: linking measurements, analyses, and models to advance the science of hydrology. *Water Resour Res* 42(3):1–5. doi:10.1029/2005WR004362
- Kura NU, Ramli MF, Ibrahim S, Sulaiman WNA, Aris AZ, Tanko AI, Zaudi MA (2015) Assessment of groundwater vulnerability to anthropogenic pollution and seawater intrusion in a small tropical island using index-based methods. *Environ Sci Pollut Res* 22(2):1512–1533
- Lavapuro M, Lipponen A, Artimo A, Katko T (2008) Groundwater sustainability indicators: testing with Finnish data. *Boreal Environ Res* 13:381–402
- Li R, Merchant JW (2013) Modeling vulnerability of groundwater to pollution under future scenarios of climate change and biofuels-related land use change: a case study in North Dakota, USA. *Sci Total Environ* 447:32–45. doi:10.1016/j.scitotenv.2013.01.011
- Lobo-Ferreira JP, Chachadi AG, Diamantino C, Henriques MJ (2007) Assessing aquifer vulnerability to seawater intrusion using the GALDIT method: part 1, application to the Portuguese Monte Gordo aquifer. In: Lobo-Ferreira JP, Ferreira, Viera JMP (eds) Proceedings water in Celtic countries: quantity, quality and climate variability, IAHS Publication 310, International Association of Hydrological Sciences, Wallingford, UK, pp 161–171
- Luoma S, Okkonen J (2014) Impacts of future climate change and Baltic Sea level rise on groundwater recharge, groundwater levels, and surface leakage in the Hanko Aquifer in southern Finland. *Water* 6:3671–3700. doi:10.3390/w6123671
- Luoma S, Pullinen A (2011) Field investigation and estimates of hydraulic conductivity from slug tests in the First Salpausselkä formation in the Santala area, Hanko, south Finland, Archived report. Geological Survey of Finland, Espoo, Finland
- Luoma S, Klein J, Backman B (2013) Climate change and groundwater: impacts and adaptation in shallow coastal aquifer in Hanko, south Finland. In: Schmidt-Thomé P, Klein J (eds) Climate change adaptation in practice: from strategy development to implementation. Wiley-Blackwell, Chichester, UK, pp 137–155
- Luoma S, Okkonen J, Korkka-Niemi K, Hendriksson N, Backman B (2015) Confronting vicinity of the surface water and sea shore in a shallow glaciogenic aquifer in southern Finland. *Hydrol Earth Syst Sci* 19:1353–1370. doi:10.5194/hess-19-1353-2015
- Mäkinen R (2008) Drinking water quality and network materials in Finland: summary report. Publications of Finnish Institute of Drinking Water 5. Finnish Institute of Drinking Water [https://www.samk.fi/download/27214\\_Summary.pdf](https://www.samk.fi/download/27214_Summary.pdf). Accessed 24 June 2014
- Mäkinen R, Orvoma M, Vejjalainen N, Huttunen I (2008) The climate change and groundwater regimes in Finland. The 11th International Specialized Conference on Watershed and River Basin Management, Budapest, Hungary, 4–5 September 2008
- Meier HEM, Kjellström E, Graham LP (2006) Estimating uncertainties of projected Baltic Sea salinity in the late 21st century. *Geophys Res Lett* 33. doi:10.1029/2006GL026488
- Millero FJ, Kremling K (1976) The densities of Baltic Waters. *Deep-Sea Res* 23:1129–1138
- Najib S, Grozavu A, Mehdi K, Breaban IG, Guessir H, Boutayeb K (2012) Application of the method GALDIT for the cartography of groundwaters vulnerability: aquifer of Chaouia coast (Morocco). *Sci Ann Alexandru Ioan Cuza Univ Iasi Geogr Ser* 58(2):77–88. doi:10.15551/scigeo.v58i2.163
- National Research Council (1993) Ground water vulnerability assessment, contamination potential under conditions of uncertainty. National Academy Press, Washington, DC, 224 pp. <http://books.nap.edu/books/0309047994/html>. Accessed December 2015
- Neumann T, Eilola K, Gustafsson B, Müller-Karulis B, Kuznetsov I, Meier HEM, Savchuk OP (2012) Extremes of temperature, oxygen and blooms in the Baltic Sea in a changing climate. *R Swed Acad Sci AMBIO* 41:574–585
- Nicholls RJ, Wong PP, Burkett VR, Codignotto JO, Hay JE, McLean RF, Ragoonaden S, Woodroffe CD (2007) Coastal systems and low-lying areas, climate change 2007: impacts, adaptation and vulnerability, contribution of Working Group II. In: Parry ML, Canziani OF, Palutikof JP, Van der Linden PJ, Hanson CE (eds) The Fourth Assessment Report of the Intergovernmental Panel on Climate Change. Cambridge University Press, Cambridge, pp 315–356
- Okkonen J (2011) Groundwater and its response to climate variability and change in cold snow dominated regions in Finland: methods and estimations. PhD Thesis, University of Oulu, Finland
- Okkonen J, Kløve B (2010) A conceptual and statistical approach for the analysis of climate impact on ground water table fluctuation patterns in cold conditions. *Hydrogeol J* 388:1–12
- Oude Essink GHP (1999) Impact of sea-level rise in the Netherlands. In: Bear J, Cheng AHD, Sore S, Quasar D, Herrera I (eds) Seawater intrusion in coastal aquifers: concepts, methods and practices, theory and applications of transport in porous media. Kluwer, Norwell, UK, pp 507–530
- Oude Essink GHP (2001) Improving fresh groundwater supply: problems and solutions. *Ocean Coast Manag* 44:429–449
- Oude Essink GHP, van Baaren ES, de Louw PGB (2010) Effects of climate change on coastal groundwater systems: a modeling study in the Netherlands. *Water Resour Res* 46. doi:10.1029/2009WR008719
- Pulido-Leboeuf P (2004) Seawater intrusion and associated processes in a small coastal complex aquifer (Castell de Ferro, Spain). *Appl Geochem* 19:1517–1527
- Rasmussen P, Sonnenborg TO, Goncear G, Hinsby K (2013) Assessing impacts of climate change, sea level rise, and drainage canals on salt-water intrusion to coastal aquifer. *Hydrol Earth Syst Sci* 17:421–443

- Recinos N, Kallioras A, Pliakas F, Schuth C (2015) Application of GALDIT index to assess the intrinsic vulnerability to seawater intrusion of coastal granular aquifers. *Environ Earth Sci* 73(3):1017–1032
- Saarnisto M, Saarinen T (2001) Deglaciation chronology of the Scandinavian Ice Sheet from the Lake Onega basin to the Salpausselkä end moraines. In: Thiede J, Bauch H, Hjort C, Mangerud J (eds) *The Late Quaternary stratigraphy and environments of northern Eurasia and the adjacent Arctic seas: new contributions from QUEEN: selected papers from the annual QUEEN workshop held in Øystese, Norway, April 1999, and in Lund, Sweden, April 2000*. *Global Planetary Changes* 31(1–4):387–405
- Sanford WE, Pope JP (2010) Current challenges using models to forecast seawater intrusion: lessons from the Eastern Shore of Virginia, USA. *Hydrogeol J* 18:73–93. doi:10.1007/s10040-009-0513-4
- Schwartz FW, Zhang H (2003) *Fundamentals of groundwater*. Wiley, New York
- STM (2001) Decree of the Ministry of Social Affairs and Health (STM) relating to the quality and monitoring of water intended for human consumption. No. 461/ 2000. <http://www.finlex.fi/fi/laki/kaannokset/2000/en20000461.pdf>. Accessed 24 June 2014
- Tarvainen T, Klein J, Jarva J, Backman B, Luoma S (2013) ESPON climate: climate change and territorial effects on regions and local economies—a final report Annex 7. Case study coastal aquifers. Applied research project 2013/1/4. Geological Survey of Finland, Espoo, Finland
- Trabelsi N, Triki I, Hentati I, Zairi M (2016) Aquifer vulnerability and seawater intrusion risk using GALDIT, GQISWI and GIS: case of a coastal aquifer in Tunisia. *Environ Earth Sci* 75(669):1–19
- Van Stempoot D, Ewert L, Wassenaar L (1993) Aquifer Vulnerability Index AVI: a GIS compatible method for groundwater vulnerability mapping. *Can Water Res J* 18:25–37
- Vrba J, Zaporozec A (1994) Guidebook on mapping groundwater vulnerability. IAH International Contributions to Hydrogeology, 16, Heise, Hannover, Germany
- Werner AD, Simmons CT (2009) Impact of sea-level rise on sea water intrusion in coastal aquifers. *Ground Water* 47(2):197–204
- Werner AD, Ward JD, Morgan LK, Simmons CT, Robinson NI, Teubner MD (2012) Vulnerability indicators of sea water intrusion. *Ground Water* 50(1):48–58
- Werner AD, Bakker M, Post VEA, Vandenbohede A, Lu C, Ataie-Ashtiani B, Simmons CT, Barry DA (2013) Seawater intrusion processes, investigation and management: recent advances and future challenges. *Adv Water Res* 51:3–26
- WHO (2011) Guidelines for drinking-water quality, 4th edn. WHO, Geneva, [http://www.who.int/water\\_sanitation\\_health/publications/dwq\\_guidelines/en/](http://www.who.int/water_sanitation_health/publications/dwq_guidelines/en/). Accessed 24 June 2014